Proceedings of ASME FEDSM'02
ASME 2002 Fluids Engineering Division Summer Meeting
Montreal, Quebec, Canada, July 14-18, 2002

FEDSM2002-31354

TURBULENCE MEASUREMENTS WITHIN A CYCLIC FLOW AND ANALYSIS IN THE MOMENTUM EQUATION

Eugene Suk[†] **Daniel K. Fetter**[‡] **Pierre E. Sullivan**[*]

Turbulence Laboratory
Department of Industrial and Mechanical Engineering
University of Toronto
Toronto, Ontario, Canada, M5S 3G8
esuk@mie.utoronto.ca[†] *dfetter1234@hotmail.com*[‡] *sullivan@mie.utoronto.ca*[*]

ABSTRACT

Particle Image Velocimetry (PIV) measurements were performed within an optical water analog engine. A unique triggering and data collection system was developed to allow a CCD camera to acquire two consecutive image frames at predetermined crank angles. The water analog engine operated at 15 RPM and had a square cross-section with two circular valved inlets. Measurements were made throughout an entire cycle to determine mean and turbulence statistics and results at 60 crank angle degree are discussed in this paper. Different averaging techniques were used and results between the techniques were compared to provide a number of statistical quantities having large discrepancies in scales and distributions. A study of the equations of motion showed that different averaging techniques results in differing physical interpretations of the flow.

NOMENCLATURE

x, y Cartesian coordinate components.
U, V Mean velocity components.
u', v' Turbulence velocity components.
P Mean pressure.
p' Fluctuating pressure.
i, j Matrix or vector component.
k Engine cycle number.
θ Crank angle.
ν Kinematic viscosity of the fluid.
ρ Density of the fluid.
DWT Discrete wavelet transformation.
CAD Crank angle degree.
RPM Revolution per minute.

Introduction

A limitation of performing PIV measurements in an engine is the need for high resolution and a large field of view, thus autocorrelation based techniques [1] are required. In autocorrelation PIV, images are doubly exposed on a single frame and the direction of flow is not easily determined due to directional ambiguity. Reuss et al. [16, 17] used a 35 mm camera and photographic film to obtain pulse separations $\Delta t = 35\ \mu s$ and a wide field of view. Nino et al. [10] used two different laser colors to eliminate directional ambiguity as the exposures could be differentiated based on color. However, good correlation was obtained between the broad features of the PIV results and the LDV or Hot–wire measurements performed by other researchers in a similar engine geometry [12] without separately colored lasers [10] or image shifting [15]. They also found that the flow was characterized by the formation of large scale vortices (tumble and swirl) which were shown to persist through the majority of the compression stroke. Reeves et al. [12] noted that a cross-correlation algorithm was necessary for significant measurements in cyclic

[*]Contact author

flows, as the directional ambiguity is removed even in strongly reversing flows.

Rouland et al. [18] used PIV in a four valve, four stroke single cylinder research engine with cross–correlation based PIV [1]. Their field of view was approximately 55 mm by 68 mm in the tumble plane and 60 mm by 60 mm in the swirl plane and a spatial separation of approximately 0.62 mm between velocity vectors allowing the collection of small scale flow characteristics. Choi [3], Denlinger et al. [5] performed 3–D particle tracking velocimetry (PTV) in a cyclic in–cylinder flow (4 valve pent roof engine) with water as the working fluid. The appearance of smaller scale flow patterns was found at higher operating speeds and that small scale motions would be important to the turbulent mixing while the large-scale structures store a great deal of kinetic energy transferred into the turbulence . Reeves et al. [13, 14] developed a high speed digital PIV system for flow visualization (pseudo particle streak) and cycle–resolved PIV data. Engine was running at the speed of 700 RPM and crank angle resolution was given as 0.467 crank angles with an imaging rate of 9000 fps (Δ t = 111 μs). Typically 20 vector fields for each cycle were collected for statistics. Ensemble averaging scheme was used to calculate the statistics such as mean velocity and RMS fluctuating turbulence. Considerable shift of center of the swirling flow for even very slight piston movement was observed and significant deviation from whole-body rotation contributed to the non-stationary characteristics in the flow. Significant out-of-plane velocity structure and strong tumbling flows also appeared. Suk et al. [20] performed PIV measurement for cyclic flow within a water analog engine operated at 15 RPM. Two consecutive singly exposed image frames were captured at a particular crank angle over 200 cycles. Ensemble averaging analysis was performed to produce a significant variation in the velocity field. A strong effect on the flow from the inlet valves resulted in the two asymmetrical oscillations in the instantaneous flow field.

There has been different methods dealing with PIV measurements data within the cyclic engine flow to decompose the mean and turbulent quantities from instantaneous velocity. Trigui et al. [23], Suk et al. [20] and Reeves et al. [14] used ensemble averaging resulting in high RMS turbulence quantities including the cycle–to–cycle mean variations (large scale) and the small scale turbulence as well possibly leading to a misinterpretation of the turbulence field within cyclic engine flow. Reuss et al. [16] performed a low–pass spatial filtering analysis to extract the cycle–resolved, large scale structures for an individual cycle and successfully reconstructed the cycle–resolved, two–dimensional velocity field based on the two–dimensional autocorrelation PIV results. Trigui et al. [22] also used a spatial low pass filtering technique to evaluate cycle–resolved large scale motion of the flow field over many cycles. The spatial cut-off of the filter was set to 1/3 of the engine bore diameter. It was argued that the use of Fourier base functions would not be optimal because the resulting decomposition was biased by *a priori* defined base functions [11].

Raposo et al. [11] used wavelet–based (DWT) averaging to decompose instantaneous non-stationary velocity records within a water analog engine with two–dimensional PIV velocity measurement. They compared the Discrete Wavelet Transform (DWT) and Proper Orthogonal Decomposition (POD) in the decomposition of instantaneous velocity to investigate the problem of cyclic variations. In the cases for the non-stationary flow due to cycle–to–cycle in–cylinder variation, the non–linear approximation given by the wavelet decomposition showed better approximate to the low wave–number field than a linear decomposition technique such as the POD. Suk et al. [19] performed a wavelet–based (DWT) averaging analysis within a cyclic flow and compared with ensemble averaging and cyclic averaging analysis. Comparison between the mean and turbulence velocities found from ensemble, cyclic and wavelet–based averaging results in differing interpretation of turbulence velocities. Cyclic averages using a uniform cut–off frequencies and ensemble average without consideration of cyclic mean variation overestimated the true turbulence and turned out to be inappropriate within the engine flow and can influence physical interpretation of engine turbulence levels and related CFD predictions.

A study of the equations of motion using a PIV measurement results was done by Li et al. [8]. Results were compared to computational work to validate the model used in the code which was k–ε model (KIVA). Very high Reynolds stress transport compared to other terms (diffusion, convection) was found in the experimental which may be due to the ensemble averaging analysis. The computational work is found not adequately capturing the higher order turbulence statistics obtained in the experimental results. The study concluded that the Reynolds stress transport is the dominant component of the equation of motion near the piston surface and causes the turbulent mixing which is responsible for the mixing and combustion efficiency in an engine.

Experimental method

Figure 1 is a schematic of the water analog engine with the particle image velocimetry (PIV) system included. The water analog engine has a 100 mm $\times$ 100 mm square inner cross–sectional area with two symmetrically located (40 mm diameter) valves that were both open 15 mm throughout the measurements. A clearance of 20 mm was used and the piston stroke was set to 75 mm. A $1/2$ horsepower direct current motor was used to drive the flow at 15 RPM. The inlet flow exceeded the Reynolds numbers examined by Durst et al. [6]. Thus the interaction of the initial vortex with the piston wall was expected to ensure transition to turbulence. Distilled water was seeded with spherical (15 μm diameter) silver coated particles with a hollow glass core and a relative density of 1.65. A square section was used to en-

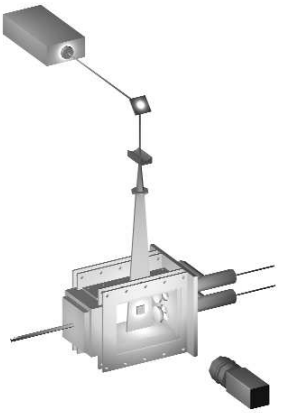

Figure 1. PIV system and the optical water analog engine

sure minimal optical distortion of the measurement region and the cell was oriented horizontally for mechanical stability. Optical access is possible with glass on all the sides for CCD camera and laser sheet

A 2-D planar PIV system with an external trigger from the water analog engine was used for the measurements. A metal obstruction on the crank wheel triggered data collection at 60 crank angle degrees (for this work) as it passed the optical sensor. This triggered a) the camera (Pulnix TM-9701) to start a new frame with an asynchronous reset, b) the two lasers (CONTINUUM MINILITE dual cavity Neodyymium-Yttruim Aluminum Garnet (Nd:YAG)) to pulse and c) the framegrabber (BITFLOW Road Runner 44) to capture the incoming camera frames. A 1 mm light sheet thickness for particle illumination was created and 162 microseconds time separation between images was allowed for in–plane motion of particles. 200 sets of images were captured for the measurement at center region, 35 mm downstream from the top of the cylinder (60 CAD).

Velocity fields were calculated using the Adaptive Cross Correlation (ACC) PIV algorithm developed by Usera [24]. The ACC algorithm is iterative and for each iteration, different interrogation area sizes (from large to small sizes) are used to be incorporated as a rough estimate of the particle displacement, thus allowing improved spatial and dynamic resolution compared to traditional cross correlation methods. Three-point Gaussian peak fitting was used for the sub-pixel analysis to improve the approximation of particle centers, increasing the accuracy of the velocity calculations. This technique fits a Gaussian function to the correlation peak using three adjoining values and gives an uncertainty level of approximately 0.1 pixels [9].

Turbulence averaging

The velocity fields were examined with two different averaging methods for the analysis; ensemble averaging, and wavelet–based (DWT) averaging. All turbulence quantities are determined by subtraction of mean values from the instantaneous values at each position.

Ensemble averaging The decomposition for the data is performed as:

$$U(\vec{x},\theta,k) = \overline{U_E(\vec{x},\theta)} + u'_E(\vec{x},\theta,k) \quad (1)$$

where $U(\vec{x},\theta,k)$ is the measured instantaneous 2D velocity in cycle k at a crank angle θ, $\overline{U_E(\vec{x},\theta)} = \frac{1}{N}\sum_{k=1}^{N} U(\vec{x},\theta,k)$ is the ensemble average over N number of data, and $u'_E(\vec{x},\theta,k)$ is the instantaneous turbulence velocity in cycle k at a crank angle θ. Problems resulting from the use of ensemble averaging include smoothing of data resulting in an over–estimation of the turbulence energy [19, 21, 2].

Wavelet averaging Wavelet–based analysis was introduced for the velocity decomposition. According to Farge [7], energy transfers driven by turbulent dynamics occur locally in both space and scale, and wavelet transformation can achieve a good performance in an energy decomposition with phase and space. Especially for non-stationary flow, separating quasi-periodic motion from cycle-to-cycle varying events, Wavelet averaging analysis is very effective. The wavelet function, ψ, acts as a high-pass filter, highlighting details of the decomposed signal. The scaling function, ϕ is a low-pass filter and produces approximations of the decomposed signal. This approach separates the velocity field with large and small scales to produce the first level approximation coefficient, $h(n)$, and first level detail coefficient, $g(n)$ [19]. This is the first level decomposition and the velocity field is separated into smooth approximations at the largest scale and details at smaller scales. The approximation coefficients will be treated as the mean component of the velocity field and the detail coefficients as the turbulence component. A Daubechies-12 wavelet was used in the study. To deal with signal-end effects involved by a convolution-based algorithm at the edges of velocity field, smooth padding of order 1 which is the first derivative interpolation at the edges is applied for two–dimensional extension. Suk et al. [19] has demonstrated improvement with Wavelet–based analysis over conventional averaging methods using 2D velocity data from PIV measurement.

Equations of motion

The data was analyzed with the Reynolds averaged equations of momentum conservation.

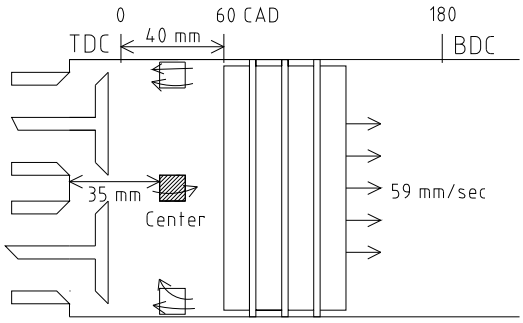

Figure 2. Ensemble mean flow at 60 CAD

Reynolds equation is given as,

$$\underset{\text{I}}{\frac{\partial U_j}{\partial t}} + \underset{\text{II}}{U_i \frac{\partial U_j}{\partial x_i}} = \underset{\text{III}}{-\frac{1}{\rho}\frac{\partial P}{\partial x_j}} + \underset{\text{IV}}{\nu \frac{\partial^2 U_j}{\partial x_i \partial x_i}} + \underset{\text{V}}{\frac{\partial \langle -u_i' u_j' \rangle}{\partial x_i}} \qquad (2)$$

where convection term (II), diffusion term(IV) and Reynolds stress transport term (V) were applied with experimental data.

Results

Velocity fields The ensemble mean velocities and ensemble mean of the DWT averages were comparable and were of similar magnitude and direction at 60 CAD as was found in the previous work [19] for other piston positions. Figure 2 shows the mean flow schematic using the ensemble velocity information to reveal two asymmetric vortices being generated by looking at the recirculation flow at the bottom and top measurement location. These vortices seem to be oscillating throughout the cycle and over the cycle, confirmed by DWT analysis, implying that the flow field is classified as non–stationary, quasi–periodic, cyclic flow.

For the turbulence, DWT results are of lower magnitude than ensemble results. The indication is that the flow field has very low order small scale mixing when interpreted with DWT averaging in comparison with the ensemble results. The DWT turbulent information (RMS value) (not presented here due to limited space) contains no spatially preferential value of RMS magnitude and is evenly distributed throughout the measurement region.

Reynolds equation Terms analyzed in the section are quantities from Eq. (2) evaluated from the 2–D planar PIV measurement results. Ensemble and DWT averaging methods are used and comparison is made between them.

Starting from the convection term, labeled II on top in Eq. (2), histograms of convection terms, $U\partial U/\partial x$, $V\partial U/\partial y$, $U\partial V/\partial x$, and $V\partial V/\partial y$ at 60 CAD using ensemble and DWT averaging methods are presented in Fig. 3 and 4. Only limited quantities are evaluated due to the limitation of 2–D planar PIV measurement only extracting the information out of the planar sheet. For both averaging methods, ensemble and DWT methods, convection terms are much higher than diffusion terms. Ensemble averaging analysis shows no comparable result between each distribution in Fig. 3 where they are even biased to different values. However, DWT averaging analysis results in all their peaks being placed close to zero. The fact that $U\partial U/\partial x$, $U\partial V/\partial y$ ($-8000 \sim 8000\ mm^2/sec$), and $V\partial U/\partial y$, $V\partial V/\partial y$ ($-2000 \sim 2000\ mm^2/sec$) have similar distribution appears to imply that mean values multiplied in each term, U and V, dominates the flow dynamics over the mean velocity gradients (see Fig. 4).

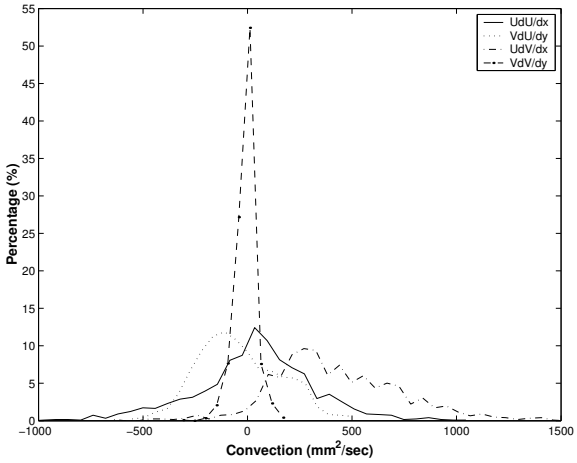

Figure 3. Convection (Ensemble)

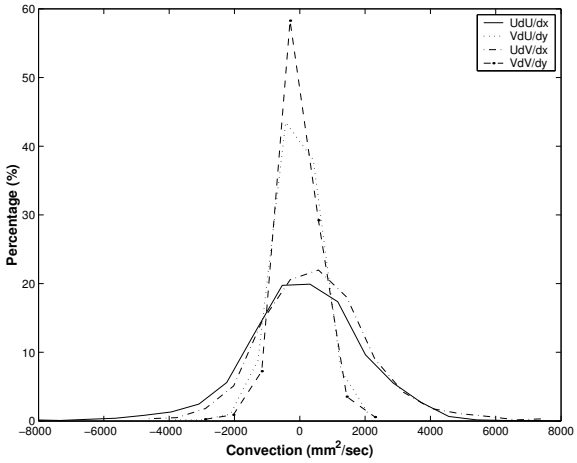

Figure 4. Convection (DWT)

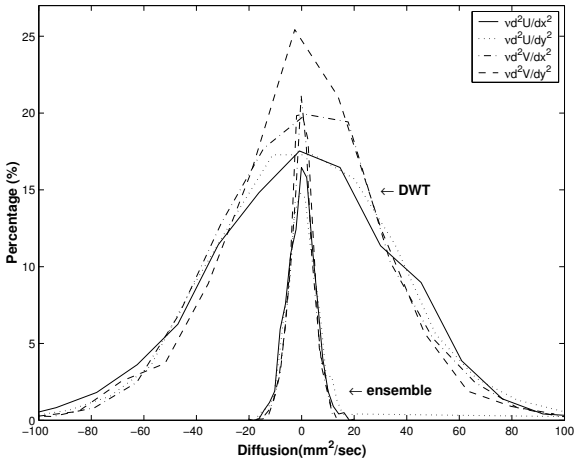

Figure 5. Diffusion terms(Ensemble & DWT)

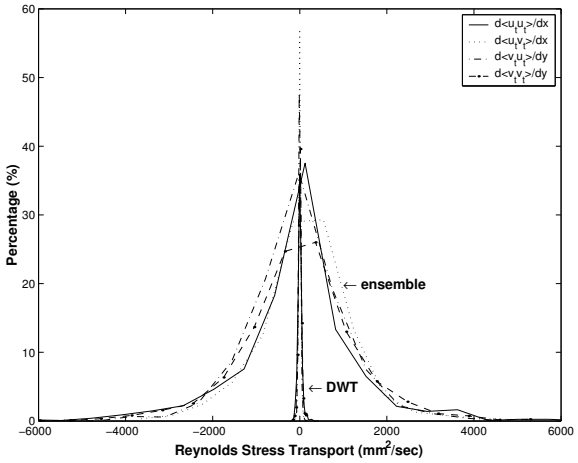

Figure 6. Reynolds Stress Transport (Ensemble & DWT)

Higher magnitude of U than V involvement should be the consequence from the consideration of early intake process. It is also noticed that for the DWT averaging, the convection term is the largest one among others (Diffusion and Reynolds stress transport).

Diffusion terms, labeled IV on top in Eq. (2) are introduced in Fig. 5. The histograms are given for each diffusion term, $\nu\partial^2 U/\partial x^2$, $\nu\partial^2 U/\partial y^2$, $\nu\partial^2 V/\partial x^2$, and $\nu\partial^2 U/\partial y^2$, for both methods. Physically, these are associated with viscous action but considering that all terms are comparable to each other, second order of gradients for both U and V are also comparable. DWT results have a wider variation ($-100 \sim 100\ mm^2/sec$) than the ensemble results ($-20 \sim 20\ mm^2/sec$) but they are significantly smaller than either convection or Reynolds stress transport.

Reynolds stress transport terms, V in Eq. (2), are introduced in Fig. 6. Reynolds stress transport, $\partial\langle -u'u'\rangle/\partial x$, $\partial\langle -u'v'\rangle/\partial x$, $\partial\langle -v'u'\rangle/\partial y$, and $\partial\langle -v'v'\rangle/\partial y$, are only available with the PIV data.

For the ensemble averaging method, Reynolds stress transport terms are the most significant term within the Reynolds equation producing variation of $-6000 \sim 6000\ mm^2/sec$. Compared to convection or diffusion phenomena, it is very significant difference. This is due to the high turbulence interpretation characteristics from the ensemble analysis where part of the large scale information is kept in the smaller scale result like turbulence. Davis [4] showed the same result of high Reynolds stress transport magnitude using the ensemble analysis within the water analog engine. On the other hand, the DWT averaging method presents very low Reynolds stress transport quantity as $-200 \sim 200\ mm^2/sec$. The value is even lower than that of the convection terms in DWT averaging, and has a same order of variation as diffusion term in DWT analysis. A study of DWT averaging with PIV measurement technique Suk et al. [19] demonstrated a lower turbulence level under 20 % as compared to ensemble averaging (over 100 % of mean value) in non-stationary, quasi–periodic cyclic flow. Thus there is a lower magnitude Reynolds stress and consequently lower magnitude Reynolds stress transport. As a consideration of an early stage of intake process in cyclic engine flow, this can be physically explained with scale evolution throughout the process. At this point more mixing is expected to correspond to larger scale flow motion of convection than smaller scale flow motion such as diffusion or Reynolds stress transport. More smaller scale motions are involved in the latter stage of the intake process, however, this does not mean that there are comparable quantities between convection and RST or diffusion at the end stage of intake process. Smaller scale motion appears to be very low in cyclic engine flow with reciprocating piston [19].

Conclusion

An experimental study was performed within a cyclic flow using PIV. Ensemble and DWT averaging methods were used to show that ensemble results have a tendency to impose significantly higher turbulence than DWT averaging. Using a ensemble averaging analysis, a study of the Reynolds equation shows the magnitude of Reynolds stress transport terms are significantly larger than the magnitude of the convection and diffusion terms where convection terms are higher than diffusion terms. However, the magnitude of the convection terms are the most effective terms among for the DWT averaging analysis and Reynolds stress transport terms had a comparable magnitude to diffusion terms, and very low order Reynolds stress transport terms.

ACKNOWLEDGMENT

The authors gratefully acknowledge the support of the Natural Sciences and Engineering Research Council (NSERC) of Canada for operating and equipment funding.

REFERENCES

[1] R. J. Adrian. Particle-imaging techniques for experimental fluid mechanics. *Annual Review of Fluid Mechanics*, **23**:pp. 261–304, 1991.

[2] R. Ancimer, P. Sullivan, and J. Wallace. Decomposition of measured velocity fields in spark ignition engines using discrete wavelet transforms. *Experiments in Fluids*, **30**:pp. 237–238, 2001.

[3] W.-C. Choi. Effects of operating speed on 3-D mean flow measured at the end of intake stroke in an IC engine. *JSME International Journal, Series B*, **41**(2):pp. 338–343, 1998.

[4] J. Davis. Investigation of Turbulent Flow in a Reciprocating Engine Using Particle Image Velocimetry. M.A.Sc Thesis, University of Toronto, 1999.

[5] A. Denlinger, Y. G. Guezennec, and W.-C. Choi. Dynamic evolution of the 3-D flow field during the latter part of the intake stroke in an IC engine. *SAE Paper*, (980485):pp. 163–173, 1998.

[6] F. Durst, T. Maxworthy, and J. C. F. Pereira. Piston-driven, unsteady separation at a sudden expansion in a tube: Flow visualization and LDA measurements. *Physics of Fluids A*, **1**(7): pp. 1249–1260, 1989.

[7] M. Farge. Wavelet transforms and their applications to turbulence. *Annual Review of Fluid Mechanics*, **24**:pp. 395–457, 1992.

[8] W. Li, P. E. Sullivan, and J. A. Davis. Comparison of experimental and computational results in a cyclic flow. Accepted by *Canadian Journal of Chemical Engineering*, January 2002.

[9] M. Marxen, P. E. Sullivan, M. R. Loewen, and B. Jähne. Comparison of Gaussian particle center estimators and the achievable measurement density for particle tracking velocimetry. *Experiments in Fluids*, **29**:pp. 145–153, 2000.

[10] E. Nino, B. Gajdeczko, and P. Felton. Two-color Particle Image Velocimetry applied to a single cylinder two-stroke engine. *SAE Paper*, (922309):pp. 1–10, 1992.

[11] J. Raposo, W. Hentschel, and W. Merzkirch. Analysis of the dynamical behavior of coherent structures in in-cylinder flows of internal combustion engines. In *10th International Symposium on Applications of Laser Techniques to Fluid Mechanics*, Lisbon, Portugal, July 2000.

[12] M. Reeves, C. Garner, J. Dent, and N. Halliwell. Particle image velocimetry measurements of in cylinder flow in a multivalve internal combustion engine. *Proceedings of the Institute of Mechanical Engineers*, **210**, 1996.

[13] M. Reeves, D. P. Towers, B. Tavender, and C. H. Buckberry. A high-speed all-digital technique for cycle-resolved 2-d flow measurement and flow visualization within SI engine cylinders. *Optics and Lasers in Engineering*, **31**:pp. 247–261, 1999.

[14] M. Reeves, D. P. Towers, B. Tavender, and C. H. Buckberry. A technique for routine, cycle-resolved 2-D flow measurement and visualization within SI engine cylinders in an engine development environment. In *10th International Symposium on Applications of Laser Techniques to Fluid Mechanics*, Lisbon, Portugal, July 2000.

[15] D. Reuss. Two-dimensional particle-image velocimetry with electrooptical image shifting in an internal combustion engine. *SPIE*, **2005**, 1993.

[16] D. L. Reuss, R. Adrian, C. Landreth, D. F. French, and T. D. Fansler. Instantaneous Planar Measurements of Velocity and Large Scale Vorticity and Strain Rate in an Engine Using Particle-Image Velocimetry. *SAE Paper*, (890616):pp. 1–25, 1989.

[17] D. L. Reuss, M. Bardsley, P. Felton, C. Landreth, and R. Adrian. Velocity, Vorticity, and Strain-Rate ahead of a Flame Measured in an Engine using Particle Image Velocimetry. *SAE Paper*, (900053):pp. 1–17, 1990.

[18] E. Rouland, M. Trinite, F. Dionnet, A. Floch, and A. Ahmed. Particle image velocimetry measurements in a high tumble engine for in cylinder flow structure analysis. *SAE Paper*, (972831):pp. 65–74, 1997.

[19] E. Suk, D. Fetter, G. Usera, and P. Sullivan. Turbulence averaging of two dimensional planar measurements within a water analog engine. Submitted in *Experiments in Fluids*, January 2002.

[20] E. Suk, P. Sullivan, and D. Fetter. PIV measurement within an optical engine. In *Flucome 2000*, Sherbrooke(QC), Canada, August 2000.

[21] P. Sullivan, R. Ancimer, and J. Wallace. Turbulence averaging within spark ignition engines. *Experiments in Fluids*, **27**: pp. 92–101, 1999.

[22] N. Trigui, W.-C. Choi, and Y. G. Guezennec. Cycle resolved turbulence intensity measurement in IC engines. *SAE Paper*, (962085):pp. 1–12, 1996.

[23] N. Trigui, J. Kent, Y. G. Guezennec, and W.-C. Choi. Characterization of intake generated fluid flow fields in IC engines using 3-D Particle Tracking Velocimetry (3-D PTV). *SAE Paper*, (940279):pp. 1–12, 1994.

[24] G. Usera. Adaptive algorithms for PIV image analyzing. Technical report, Institute of Fluid Mechanics and Environmental Engineering IMFIA, University the Republic, 1999.